Pergamon

Deep-Sea Research I, Vol. 41, No. 10, pp. 1527–1550, 1994

0967–0637/94 $7.00+0.00

What forces the variability of the southwestern Atlantic boundary currents?

SILVIA L. GARZOLI* and CLAUDIA GIULIVI†

(*Received* 11 *January* 1993; *in revised form* 14 *September* 1993; *accepted* 17 *September* 1993)

Abstract—A marked variability in the location of the front originating at the confluence of the Brazil and Malvinas Currents has been observed from both surface and subsurface observations. Modeling experiments using climatological winds predict a seasonal variability on the latitude of separation of the Brazil Current from the coast. During the Confluence Program (November 1988–February 1990) and from data collected with an array of inverted echo sounders, the location of the confluence front and its variability was established. In this paper, the observed oceanic variability is analyzed simultaneously with the wind product from the European Center for Medium Weather Forecast (ECMWF) obtained for the period of the observations. The ECMWF data is validated against *in situ* indirect wind magnitude observations obtained from a sub-array of the Confluence deployments. The large-scale anomalies are explored through the comparison with the climatological winds field obtained from HELLERMAN and ROSENSTEIN (1983), *Journal of Physical Oceanography*, **13**, 1093–1104. From the analysis it is concluded that the main source of variability of the Confluence front is the local wind forcing. There is a variability in the location of the front due to the seasonal cycle of the winds in the South Atlantic. In addition to this seasonal variability, the latitude of separation of the Brazil Current from the coast presents a marked interannual variability that is forced from anomalous wind patterns south of the Confluence. There is no apparent correlation between wind-forced pulses in the Antarctic Circumpolar Current and the observed anomalous northward penetration of the Malvinas Current.

1. INTRODUCTION

THE circulation in the southwestern Atlantic is characterized by the encounter between the warm southward flowing Brazil Current and the cold northward flow of the Malvinas Current. This encounter takes place at approximately 38°S, causing a strong thermohaline front that has been named of the Confluence front (GORDON and GREENGROVE, 1986).

A marked variability in the location of the Confluence front has been characterized from both surface (OLSON *et al.*, 1988) and subsurface observations (GARZOLI and BIANCHI, 1987; GARZOLI and GARRAFFO, 1989). In both cases it has been attributed to a variability in the latitude of separation of the Brazil Current from the coast. Satellite images indicate that during the austral summer (January, February, March) the Brazil Current reaches its southernmost extension while the Malvinas Current retreats (OLSON *et al.*, 1988; GARZOLI *et al.*, 1992). An opposite situation is observed during the austral winter (June, July,

*Lamont-Doherty Geological Observatory of Columbia University, Palisades, NY 10964, U.S.A.
†Servicio de Hidrografía Naval, Buenos Aires, Argentina.

August) when Malvinas waters invade the area and reach the northernmost latitudes. Significant interannual variability has also been observed (OLSON *et al.*, 1988; GARZOLI, 1993).

The Brazil Current is one the weakest western boundary currents (i.e. EVANS and SIGNORINI, 1985; PETERSON and STRAMMA, 1990; GARZOLI, 1993). If oceanic circulation is explained by the Sverdrup closure of the wind stress, all western boundary currents should have the same intensity. All observational evidence indicates that this is not the case; the Brazil Current transport is less than one third of the Gulf Stream. STOMMEL (1965) suggested that the cause of the differences between the Brazil Current and Gulf Stream transports could be found in the thermohaline circulation. Thermohaline circulation will enhance the Gulf Stream transport in the North Atlantic and diminish the one carried by the Brazil Current in the South Atlantic. On the other hand, one of the most important sources of forcing for the upper ocean circulation is the momentum flux imparted by the wind. Being a weak current, the wind stress can play an important role in determining the intensity of the Brazil Current transport (GORDON and GREENGROVE, 1986; OLSON *et al.*, 1988). The basin-wide average of the zonal wind stress curl shows that the low latitudes in the basin are dominated by an annual cycle in the wind stress curl (OLSON *et al.*, 1988). South of 25°S a semi-annual component is superimposed. The annual cycle apparently follows the alternative pattern of southward penetration of the Brazil Current previously described. OLSON *et al.* (1988) suggested that variations in the Brazil–Malvinas Confluence might be driven by changes in the Malvinas transport, which in turn are forced by variations in the Antarctic Circumpolar Current. GARZOLI and GARRAFFO (1989), in a study made with inverted echo sounders, suggested that the cause of the variability in the location of the Confluence front could be related to either an intensification of the winds in the Southern Ocean, or to the variability in the South Equatorial Current (SEC). PETERSON (1988) observed a direct relation between the magnitude and pulses of the winds in the Southern Ocean and the transport of the Antarctic Circumpolar Current (ACC). Since the Malvinas Current is a branch of the ACC, the variability induced by the winds in the ACC, should be reflected in the intensity and variability of the Malvinas transport.

In addition to observational studies, some modeling efforts were conducted in the region using climatological wind forcing. An analysis of a general circulation model forced with these winds (SEMTNER and CHERVIN, 1992) reproduces (with less intensity) the seasonal variability of the latitude of penetration of the Brazil Current (GARZOLI *et al.*, 1992). A regional numerical model for the South Atlantic, forced with climatological winds (MATANO *et al.*, 1992), correlates the transport of the Brazil Current and the wind stress. According to Matano *et al.*, the Brazil transport follows a perfect annual cycle directly correlated to the cycle of the curl of the wind stress in the basin. The hypothesis postulated by MATANO *et al.* (1992) is that "during the austral summer a southward displacement of the latitude of the Confluence is coincident with an acceleration of the flow in the subtropical gyre and a weakening of the transport of the Malvinas Current". That is to say, models forced with monthly averages of climatological winds reproduce an annual cycle of the frontal variability.

During 1988–1990 an extensive field work was performed to study the dynamics of the Confluence (CONFLUENCE PIs, 1990). As part of this experiment, an array of 10 inverted echo sounders was deployed with the objective, among others, to study the time space variability of the Confluence front (Fig. 1). GARZOLI (1993), based on the data collected with the inverted echo sounders array, has described the large variability observed in the

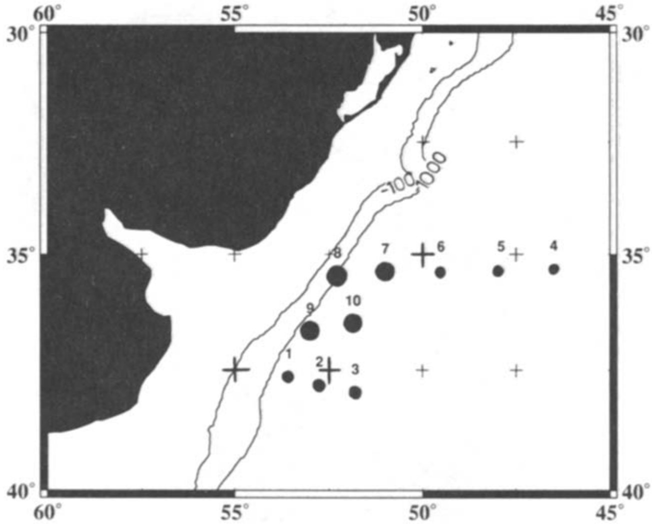

Fig. 1. Location of the Confluence array of inverted echosounders (•), inverted echosounders equipped with an ambient noise detector (●), ECW grid location (+) and ECW grid location used for the comparison (**+**).

dynamic height field and estimated geostrophic transports associated with the main flows. Most of the variability is attributed to changes in the latitude of separation of the currents, the meandering of the Confluence front towards the east, and eddy generation. Bianchi and Garzoli (submitted), using the same data set, described the temporal evolution of the frontal motions from the analysis of synoptic maps of integrated temperature in the area.

In this paper, the observed oceanic variability is analyzed simultaneously with the European Center for Medium Weather Forecast (ECMWF) winds obtained for the period of the observations. The ECMWF data is validated against *in situ* indirect wind magnitude observations obtained from a sub-array of the Confluence deployments consisting of bottom deployed ambient noise recorders. The large-scale anomalies are explored through the comparison with the climatological winds field obtains from Hellerman and Rosenstein (1983).

2. THE DATA

The oceanic data and its variability

During November 1988 an array of 10 inverted echo sounders (IES) was deployed in the area of the Brazil–Malvinas Confluence (Fig. 1) and recovered, after a period of 16 months, during February 1990 (Garzoli *et al.*, 1991). The IES is a bottom-deployed instrument designed to measure the travel time of an acoustic signal from the ocean bottom to the surface and back (Watts and Rossby, 1977). The travel time is inversely proportional to the sound velocity, which is a function of the temperature and salinity of the water column. Using the confluence CTD data (Charo *et al.*, 1991; Garzoli *et al.*, 1991) the travel time series has been sealed to dynamic height and the transects analyzed in terms of geostrophic velocities and transports (Garzoli, 1993). In this analysis it was concluded that there is a large spatial and temporal variability in the area due to the

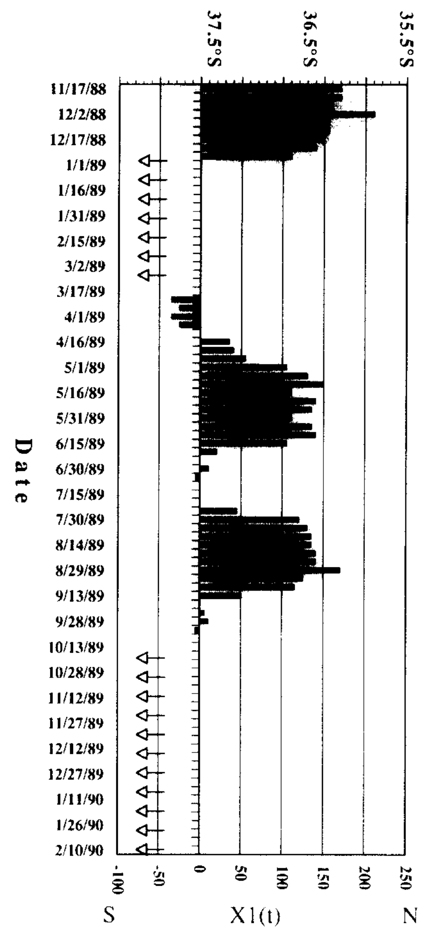

Fig. 2. Meridional displacement of the Brazil–Malvinas Confluence front, adapted from BIANCHI and GARZOLI (1993). The arrows indicate that the front was located south of the range of detection with the present array.

meandering of the Confluence front, eddy generation and frontal motions. Significant interannual variability is observed in the velocity field.

The spatial variability with time of the Confluence front was studied by BIANCHI and GARZOLI (1993). In this study, the time series of travel time obtained with the IES array were scaled to integrated temperature T_{500}. From the Confluence CTD data it was determined that low values of T_{500} (from 4° to 5°C) correspond to subantarctic water and high values of T_{500} (larger than 15°C) corresponds to subtropical waters (BIANCHI *et al.*, 1993). After smoothing the series through a process of 5-day averages, synoptic maps of T_{500} as a function of latitude and longitude were composed. These maps were analyzed and as a result, time series for east–west and north–south motions of the front were obtained. The meridional displacements are shown in Fig. 2. During the observed period, three northward intrusions of the Malvinas Current can be observed, in each of which the current reaches latitudes up to 36°S. The period of each event lasts approximately 2 months, and no apparent periodicity is observed. During November–December 1988 the

Table 1. *Characteristics of the regression between NSL and wind magnitude* (W)

IES #	Depth (m)	A	B	ε	R^2
7	3018	1.3637	−55.712	0.93	0.982
8	2231	0.9511	−27.296	1.04	0.954
10	3307	1.378	−59.646	0.59	0.959

The columns indicate respectively: the IES location, its depth in m, the coefficients a and b of the regression 20 Log W (m s^{-1}) = A NSL + B, the standard error of the estimate in m s^{-1}, and the square of the coefficient of determination R^2.

Malvinas Current reaches latitudes north of 36.5°S; for the same period of time during the following year, the current does not reach the area of the observations (i.e. it is located south of 38°S). This interannual variability is in agreement with results obtained for the velocity field by Garzoli (1993).

Wind magnitude from ambient noise measurements

Four out of the 10 IES deployed in the region were equipped with an ambient noise recorder to register the noise in the water column (Fig. 1). This provides a simple method of measuring the magnitude of the wind speed over the oceans (Lemon, 1984). The sampling resolution is 1 h at the four sites. Similar data was previously analyzed at the Confluence by Garzoli and Clements (1986) and by Garzoli and Simionato (1990). In the first analysis, a comparison between inferred winds and winds from the National Meteorological Tropical Strip Surface Analysis product, established a good agreement between both observations. In the second one, it is shown that the wind spectra from data series inferred from ambient noise measurements presents the typical characteristics of the spectra of the winds at mid-latitudes.

The calibration of the data collected with the ambient noise detectors consists of two parts. The first calibration is inherent to the instrument and determines the noise spectral level (*NSL*) from the measured voltage (Maccio, 1986). Through the second calibration, the magnitude of the surface wind speed (W) is obtained by a linear least-square fit between NSL (in dB re 1mPa) and wind speed magnitude (W) in m s^{-1}. Direct wind observations were obtained during the three cruises: one after deployment of the instruments (November 1988), one while the instruments were deployed (September 1989), and one preceding the recovery of the instruments during the final cruise (February 1990). The collected *in situ* data are used to obtain the relation between *NSL* and W. The relation between the observed ambient noise level (*NSL*) and the magnitude of the wind (W) at the surface follows the form

$$20 \log W = A\,(NSL) - B$$

(Shaw *et al.*, 1978; Evans *et al.*, 1984; Lemon *et al.*, 1984) where A and B are the coefficients of the linear regression between wind magnitude (W) and *NSL*. Since the instruments were deployed at different depths (Table 1) and used different cards, a separate linear fit was obtained for each site. The cards used on IES#7, 9 and 10 are the same series. A good correlation was obtained between on-deck wind observations and

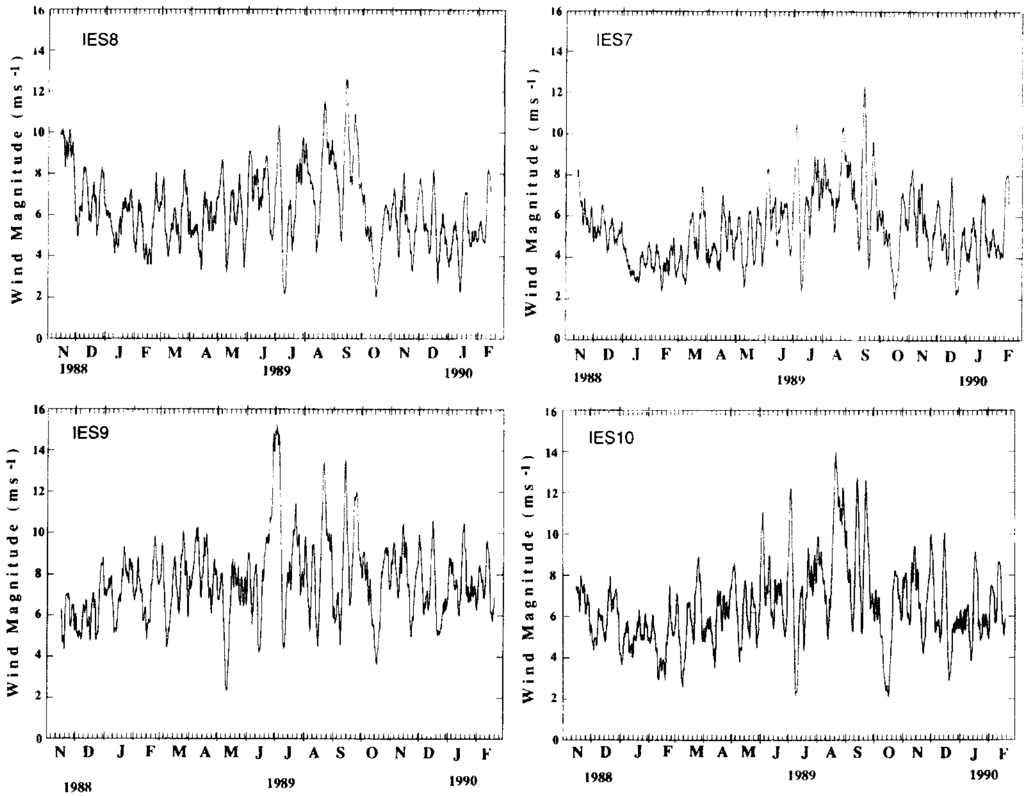

Fig. 3. Time series of the wind magnitude obtained with the NSL at the four locations indicated in Fig. 1.

NSL for sites 7, 8 and 10. Unfortunately, due to lack of direct wind measurements during the period 1989, it was not possible to obtain an individual relation for site 9. The few available observations fit the relations obtained for 7 and 10, and it was decided to use the calibration at site 10 to obtain a relation between *NSL* and *W* at site 9. Table 1 shows the parameters for the different calibrations and their statistics. By applying these relations, time series of wind magnitude are obtained at the four sites. Results are shown in Fig. 3; the series are presented as 5-day running mean of the hourly records.

The time series obtained at 35°S (IES 8 and 7) are very similar. In both cases winds are low during the SH summer and high in the SH winter. These two series are also very similar to those obtained at the southern offshore location (IES 10). Periods of high winds are observed for July, August and September at all sites. The only series that is somewhat different is the one obtained at the southern onshore site (IES 9). Winds at IES 8 and IES 9 are practically the same from 15 July 1989 to the end of the record. The high winds observed from 15 June to 15 July 1989 at IES 9 (W = 15 m s^{-1}) are not as high as IES 8. And, previous to 1 July 1989 the low frequency trend of the series is out of phase. The series obtained at IES 9 are the only ones collected in a different oceanic regime. While the other stations are almost always on Brazil Current waters, station IES 9 changes from Brazil Current waters to Malvinas Current waters as the Confluence front moves.

The European Center for Medium Weather Forecast (ECMWF) Winds

Data from the ECMWF (Trenberth and Olson, 1988a,b,c; Trenberth, *et al.*, 1989; Halpern *et al.*, 1992) were made available for the present study by the National Center for Atmospheric Research (NCAR). Trenberth and Olson (1988a, b, c) analyzed this data set and concluded that it is the best operational model generated wind. For the northern hemisphere, Kalnay *et al.* (1990) showed that the errors of the 1-, 3- and 5-day forecasts were smaller than those obtained from the National Meteorological Service. Surface wind components at 10 m height were issued twice a day in a 2.5° × 2.5° grid, at 0000 and 1200 GMT for the period of the IES observations.

From the U and V components of the daily winds, the wind magnitude, $W = |U^2 + V^2|^{1/2}$, is obtained and compared to the ambient noise series. The atmosphere forces the ocean through the surface wind stress. The wind stress is defined by the relation $\tau = \rho_o C_D \mathbf{W}|\mathbf{W}|$, where ρ_o is the air density and C_D is the drag coefficient. From both theory and observation it is concluded that C_D depends on the wind speed and atmospheric stability (Large and Pond, 1981, 1982). A considerable scatter exists in experimental results, leaving considerable uncertainty in C_D estimations (Trenberth *et al.*, 1989). Therefore, based on the assumption that for low frequency fluctuations (periods larger than 10 days) C_D is a constant (Willebrand, 1978), in this paper the pseudo wind stress is utilized. The pseudo wind stress is defined as the square of the magnitude of the wind and, therefore, its components are given by:

$$P\tau_x = U|U| \quad \text{and} \quad P\tau_y = V|V|$$

where U and V are the eastward and northward components of the wind respectively.

3. COMPARISON BETWEEN THE NSL AND ECMWF WIND SERIES

The series of wind magnitude obtained at the IES sites provide excellent resolution on time but poor spatial coverage. In this section, the series of NSL wind are compared with wind series from ECMWF in order to validate the model product and use it as the large-scale forcing.

The comparison is made between the average of the four series of NSL winds (NLW) and the average of the ECMWF winds (ECW) at 35.00°S 50.00°W; 35.00°S 52.5°W; 37.5°S 52.5°W and 37.5°S 55.0°W (Fig. 1). Results (Fig. 4) show the 10-day running mean of the original ($\Delta t = 1$ h) values. The series of *NLW* are sub-sampled to match the *ECW* product sampling (two values per day at 0000 and 1200 h). Statistics of the series are obtained for the overlapping time period. Results from the cross-spatial analysis between the ANW and ECW series (not shown) indicate that for periods longer than 3 days the two products are highly correlated (>0.8). The phase spectrum presents a slow shift towards higher periods. The most significant coherence is centered at 11 days (0.95) with a phase of 22° (±3°). No significant coherence is observed for periods shorter than 2 days. The coefficient for correlation between the NLW and ECW series is 0.95. The mean and the standard deviation are 6.44 m s^{-1} (1.23) and 6.73 m s^{-1} (1.01) respectively. The agreement, in general, is very good. The difference in the mean values is lower than 0.3 m s^{-1} (or less than 5% of the total signal). The standard deviation shows that the variability with respect to this mean is larger in the NLW. Differences might be attributed to the difference in the location of the NLW and ECW series averaged to the effects of the comparison (Fig. 1).

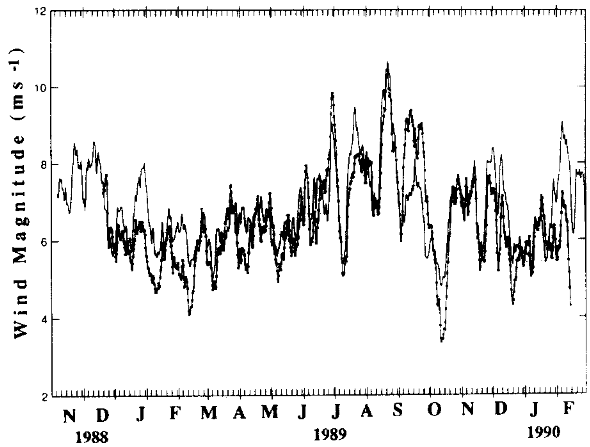

Fig. 4. Comparison between the wind magnitudes obtained from the NSL observations (dotted line) and the ECW (solid line) product. Results are given as a function of time for the period of the observations.

The main discrepancy in magnitude is observed during the SH summer of 1988 and October 1989 (Fig. 4). The similarity of the monthly oscillations observed during the southern hemisphere winter in both wind products is remarkable. The amplitude of the oscillations, in general, is larger in the NLW. This is to be expected because of better sampling time resolution in the NLW observations. Also, because most of the input to the model from which the series of the ECW are obtained comes from coastal stations and therefore prediction of the storms in open seas might be underestimated.

From this analysis it is concluded that the agreement between the two products is very good. The differences can be attributed to the spatial averaging of the wind products. Data from the ECMWF will be used in what follows as the large-scale wind forcing in the South Atlantic.

4. THE WINDS AND FRONTAL MOTIONS

In the introduction, the mechanisms responsible for the variability of the South Atlantic western boundary current system were summarized as: the acceleration of the South Atlantic subtropical gyre due to the basinwide integrated forcing, and/or pulses in the Malvinas Current transport due to an intensification of the winds in the Southern Ocean. To date, no direct comparison has been made between simultaneous wind and oceanic data to prove any of these theories. In this section, the location of the Confluence front (Fig. 2) will be compared with simultaneous ECW wind measurements to determine any possible relation between the atmospheric forcing and the position of the Confluence front.

The large-scale historical wind curl field is obtained from the HELLERMAN and ROSENSTEIN (1983) climatological wind stress monthly means. To compare with results previously published by HELLERMAN and ROSENSTEIN (1983), a similar four-point smoothing was applied to the curl of the wind stress.

To determine any possible relation between the frontal motions and the wind stress variations over the South Atlantic, the curl of the wind stress is averaged longitudinally

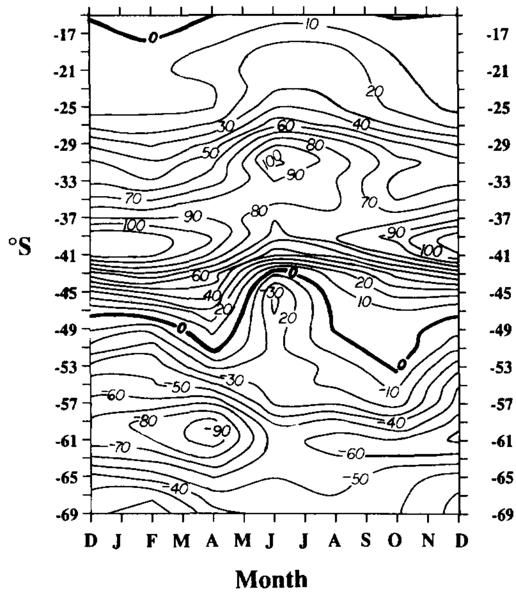

Fig. 5. Curl of the wind stress obtained from Hellerman and Rosenstein's climatological winds integrated across the South Atlantic basin as a function of time. Stress curls are given in unit of $10^{-9}\,N\,m^{-3}$.

across the whole basin from the eastern boundary (Sverdrup transport) (Fig. 5). According to Fig. 5, the wind stress in the South Atlantic follows an annual cycle. At the Confluence (37°–45°S) the curl is maximum from September through March and minimum from May through September. The opposite holds true north of the Confluence (29°–37°S). If the location of the front follows the annual cycle in the magnitude of the wind stress as suggested by models (i.e. MATANO, in press), then the Malvinas Current should be at its southward location during the southern hemisphere (SH) summer months (January, February and March); it will move northward during the SH fall (March, April and May), remain at its northward position during the SH winter (June, July and August), and return to the south during the SH spring (September, October and November). If this formulation is followed, the frontal motion (Fig. 2) presents two main discrepancies: the first one is observed during November 1988 and the second one during July 1989. The two situations will be discussed and analyzed in the following sections.

The large-scale wind during 1988–1990

Following the same procedure utilized to obtain the integrated wind stress curl for climatology, the pseudo wind stress curl is obtained from the monthly averages of the twice-per-day pseudo wind stress values of the ECW. The analysis of the zonal pseudo wind stress curl variability across the basin is repeated for the period October 1988–March 1990. Results are given in Fig. 6. It must be noted that differences in the magnitudes are due to the fact that for climatology, the variable represented is the wind stress while for the ECW the analysis is the pseudo wind stress. These values are from 1.3 to 2 times smaller than the wind stress.

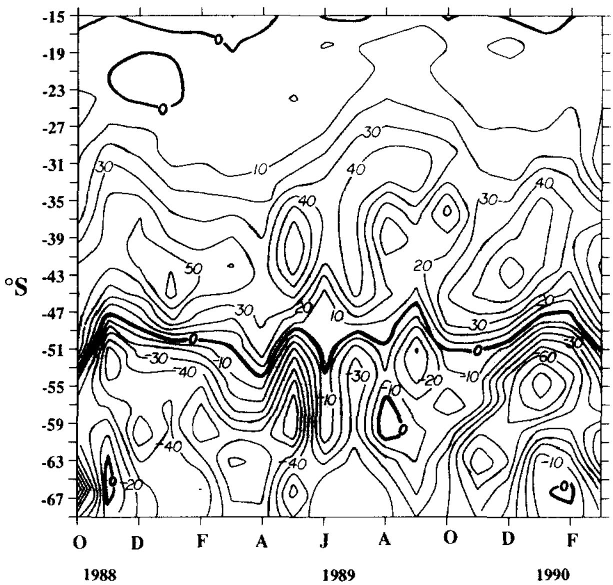

Fig. 6. Same as Fig. 5 for wind curls obtained from the ECW for the period October 1988–March 1990.

As to be expected, the ECW winds curl field (Fig. 6) is not as smooth as climatology (Fig. 5). Nonetheless, the fields present similar characteristics. The lower zero of the curl line varies between 53° and 47°S and between 53° and 43°S for climatology. The maximum values for the curl for the period October 1988 to February 1990 are centered at 43°S during January 1989, move northward and reach 31°S during August 1989 and are back at 41°S during December of the same year, following an annual cycle similar to climatology for latitudes between 29° and 43°S. South of the zero curl line larger differences between climatology and the 1988–1989 product are observed. While climatology shows two extended negative values along 61°S with a clear annual signal, the ECW presents instead a series of minimums at latitudes that vary from 51° to 63°S, with higher frequency of occurrence.

From the comparison between the distribution of the integrated zonal stress curl across the whole Atlantic basin (Fig. 6) and the simultaneous motions of the front (Fig. 2), there is no apparent relation between the expected seasonal variability forced by the acceleration of the gyre and the observed frontal location. That is to say, discrepancies between the predicted and observed locations of the front are not the result of the basin-wide integrated wind fields for the period of observations. In what follows, the analysis will focus on the regional wind patterns.

The "anomaly" of November 1988

During November–December 1988, the Malvinas Current was at its northward location while during November–December 1989 it was confined to the south. These results (Fig. 2) were obtained through measurements of integrated temperature (Bianchi and Garzoli, 1993) and confirmed by satellite images. An example is presented in Fig. 7 which shows the

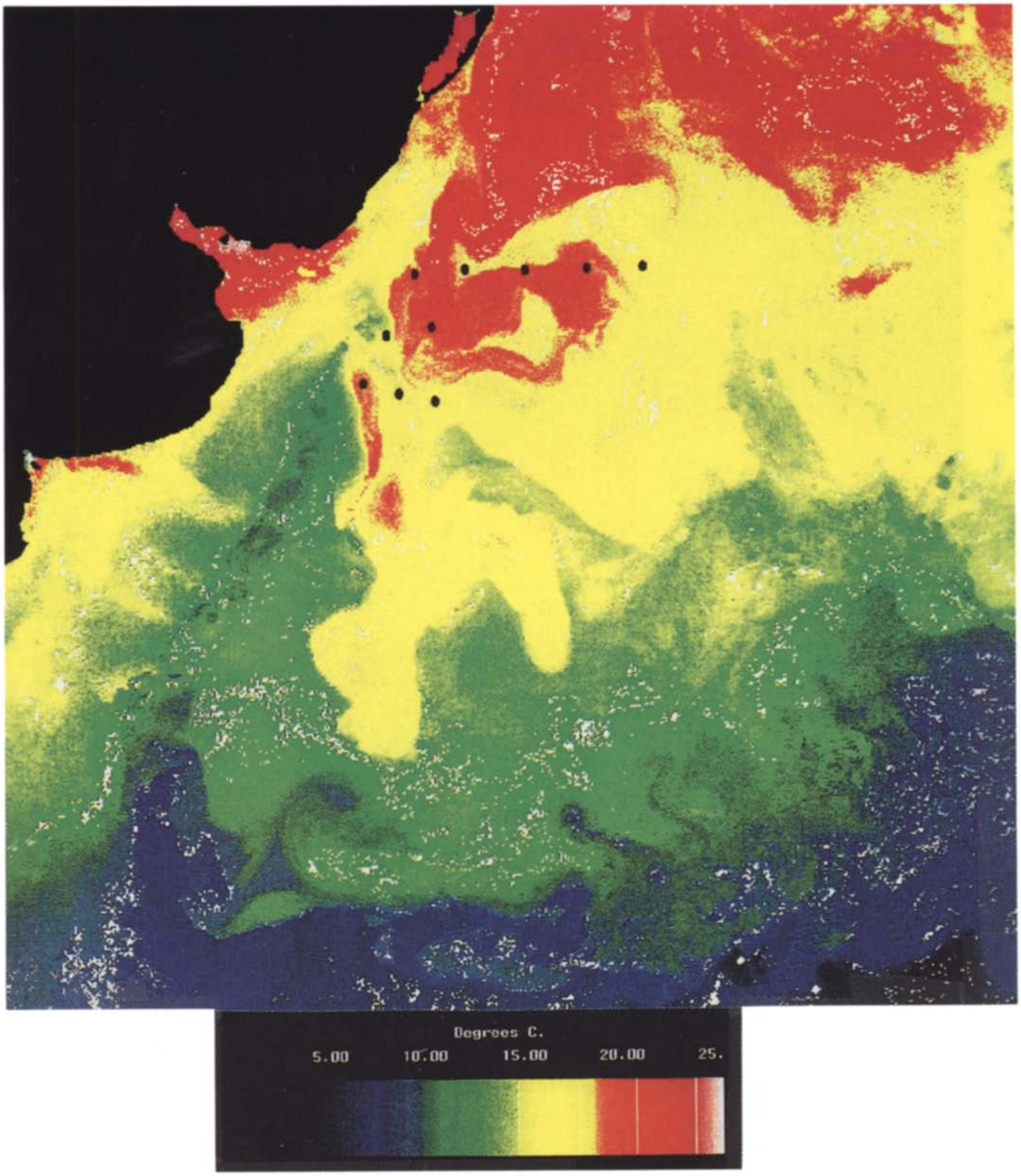

Fig. 7. NOAA/AVHRR satellite images for (a) 17 December 1988 and (b) 30 December 1989 (Podesta and Olson, personal communication). Superimposed are the locations of the IES stations.

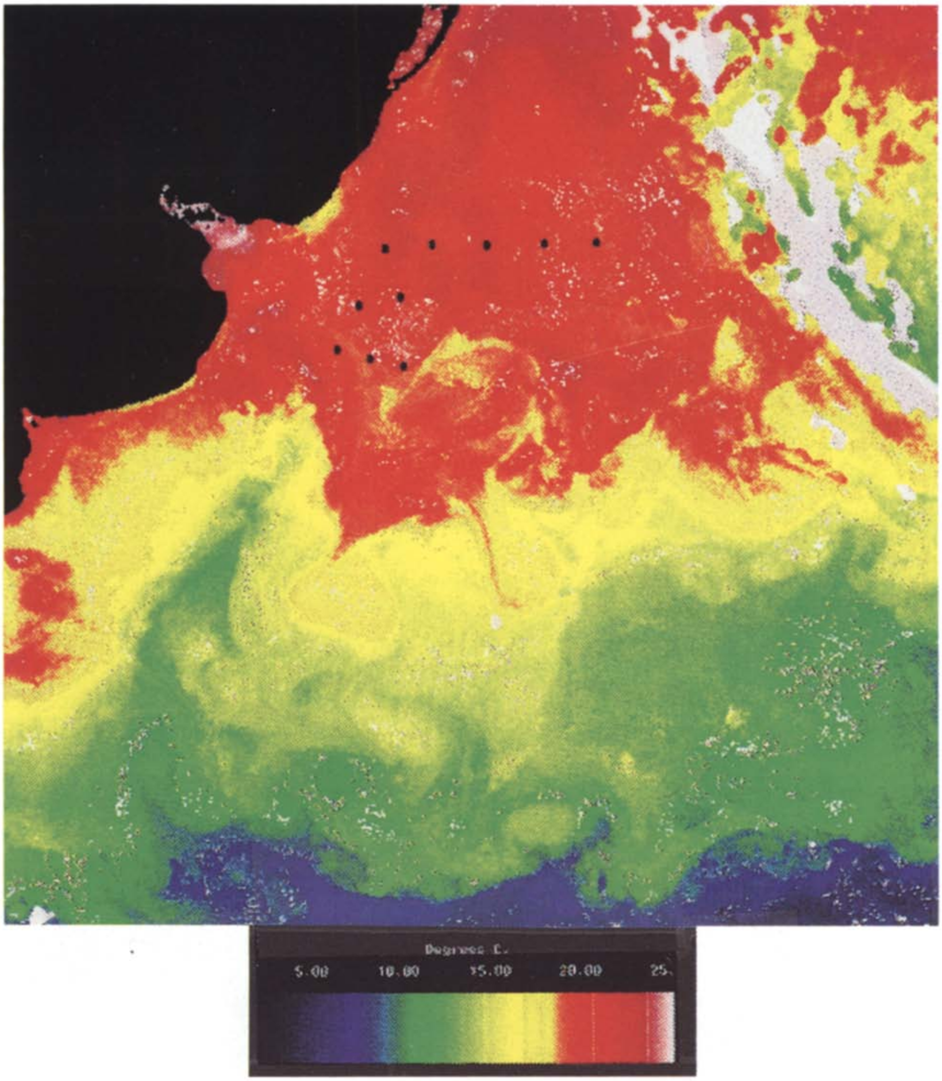

Fig. 7. *Continued*.

sea surface temperature for 17 December 1988 (Fig. 7a) and 30 December 1989 (Fig. 7b). While during 1988 values of cold sea surface temperature (SST) associated with the Malvinas Current are observed north of the Rio de La Plata (35°S) and the northern line of deployments, during 1989 the Malvinas Current is observed south of the southern line of deployments. A comparison with results from the analysis of 7 years of sea surface temperature (SST) from satellite images (GARZOLI *et al.*, 1992) indicates that the situation observed during 1989 is in agreement with the satellite observations. Also, climatological winds indicate that the maximum value of positive curl occurs during December, farther south than in July (Fig. 5). A positive curl between 35° and 40°S will accelerate the flow counterclockwise over that region, and therefore the Brazil Current will be stronger and penetrate further south. This implies a retreat of the Malvinas Current. That is to say, when compared with the different climatologies (satellite images of SST and historical winds), the situation observed during 1989 is "normal". The question that arises is why the situation during the same period of time is different one year earlier?

It has been postulated that pulses in the zonal wind component across the Drake Passage are related to pulses in the ACC (PETERSON, 1988). The Malvinas Current is a branch of the ACC, and therefore these pulses might increase its strength. This will result in a northward penetration. To determine if the "anomaly" of November 1988 is due to one of these pulses the first comparison is made between the winds in the Drake Passage and the location of the front (Fig. 2). The time variation of the wind components of the ECW averaged across the Drake Passage (65°W; 55° to 65°S) is given in Fig. 8. The series are the result of a 10-day running mean of the original data. The dominant component is the zonal. There is an onset of the zonal winds that occurs at approximately 3-month intervals. While the pulse of 1 November 1988 could be considered responsible for the northward penetration of the Malvinas Current, at the same time of the year (Fig. 2) the second pulse occurs during 1 February 1989 when the current retreats. The same is valid for the two subsequent pulses of May and September. Visual as well as statistical analysis (not shown) between the series indicates no lag correlation at this or other frequencies. Therefore, pulses of the zonal wind at the Drake Passage that force the ACC with the same periodicity cannot be related in this case to the observed northward penetration of Malvinas Current.

The same analysis is repeated for the wind components integrated across the entire ACC (0°–360° longitude). Results integrated across the Drake Passage (55°–65°S) (Fig. 9) show that the pulses are less pronounced, but that the onset occurs at approximately the same time as the series across the Drake Passage (Fig. 8). Most of the energy is in the zonal component (Fig. 9a), and the contribution of the meridional winds (Fig. 9b) is considerably smaller. Also, the variability is at higher periods. An analysis of the auto-correlation of the integrated series and cross-correlation between the integrated series (0°–360° in longitude) at different latitudes (not shown) indicates two dominant oscillations: at 70 days and 7 months. Again, there is no apparent relation between these pulses and the northward penetrations of the Malvinas Current.

The wind field is now analyzed in a regional scale. The next set of figures (Fig. 10a–c) compares the monthly mean values of the local wind stress for the months of October 1988 and 1989 and for climatology; that is to say, for the month prior to the event observed in the ocean. Overlapped is a schematic of the location of the Malvinas Current which flows northward following the topography. As the comparison is made between the pseudo wind stress and the wind stress, the magnitudes in the climatological and 1988–1989 figures are different.

Significant differences are observed in the wind stress curl distribution for the months of October 1988 and 1989 (Fig. 10). The climatological local distribution of the wind stress during the month of October (Fig. 10a) shows that the Brazil Current, as well as the core of the Malvinas Current for latitudes between 40° and 50°S are in an area where the curl is positive. Also positive is the curl in the northern side of the Drake Passage. This will result in an intensification of the southward flow and in a deceleration of the northward flow. As a consequence, the Malvinas Current will retreat. This situation is repeated during October 1989 (Fig. 10c). In contrast, during October 1988 (Fig. 10b), higher values of negative curl are observed upstream of the Malvinas Current. This negative curl will accelerate northward flow resulting in a northward penetration of the Malvinas Current.

To follow further the evolution of the 1988 event, the same analysis is performed for 10-day averages of the pseudo wind stress curl (Fig. 11). At the beginning of October (days 1–10, 1988; Fig. 11a), at the location of the Malvinas Current, between 40° and 58°S, the atmospheric circulation is mostly anticyclonic. A cyclonic motion starts to emerge from the Drake Passage. By the end of October (days 21–31, 1988; Fig. 11b) the zero curl has moved northward and is located around 45°S. This cyclonic motion will strengthen the northward flowing Malvinas Current. After than, it starts moving southward (not shown) and is close to 50°S by the end of November (days 21–31, 1988; Fig. 11c). At the beginning of January (days 1–10, 1989; Fig. 11d) the line of zero curl is at its southward position. The observed values of positive curl of the wind stress in the area increase the strength of the Brazil

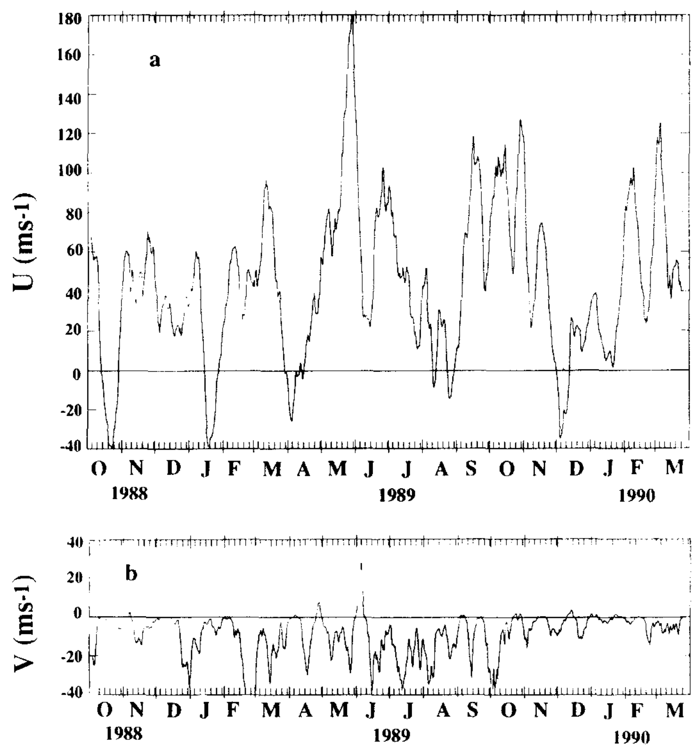

Fig. 8. (a) Zonal and (b) meridional components of the ECW integrated across the Drake Passage (55°–65°S along 65°W).

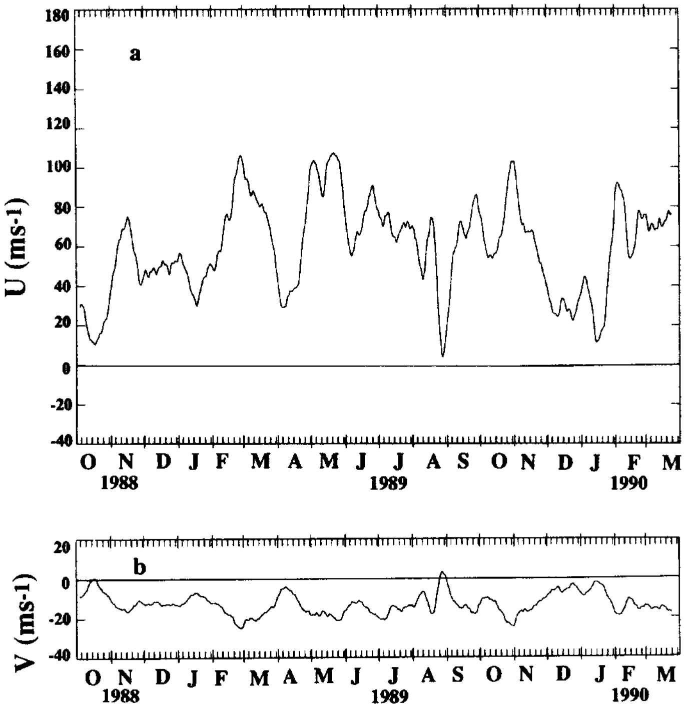

Fig. 9. (a) Zonal and (b) meridional components of the ECW integrated across the entire ACC (0°–360° in longitude) and across the Drake Passage (55°–65°S along 65°W).

Current, while they will decrease the northward flowing Malvinas Current. The result is a retreat of Malvinas as described in Fig. 2.

To verify further that the anomalous penetration of the Malvinas Current at the end of 1988 is the result of local forcing and not of the net mass balance of the basin, a comparison is made for integrated values of the local curl (zonal average between 30° and 60°W) and along the whole basin (from the eastern boundary to 70°W) (Figs 12 and 13). There is a strong similarity between the distribution of the curl of the wind stress integrated across the whole basin (Fig. 12) for the months of October 1988 and 1989 as well as climatology. In contrast, when the integration is made locally (Fig. 13) at the location of the Malvinas Current (45°–55°S), the curves corresponding to October 1989 and climatology are in phase and, in turn, out of phase with October 1988.

That is to say, there is a considerable interannual variability between the two observed periods from October to January. According to different climatologies and models, the situation during 1989 is the one to be expected. The analysis of the local winds for 1988 and 1989 indicates that this anomalous northward migration of the Malvinas Current observed during 1988 might be due to interannual variability of the winds south of the Confluence.

The "anomaly" of July 1989

Another apparent anomaly is a southward penetration of the Brazil Current (or retreat of the Malvinas Current) during July 1989. All previous studies indicate that the Malvinas

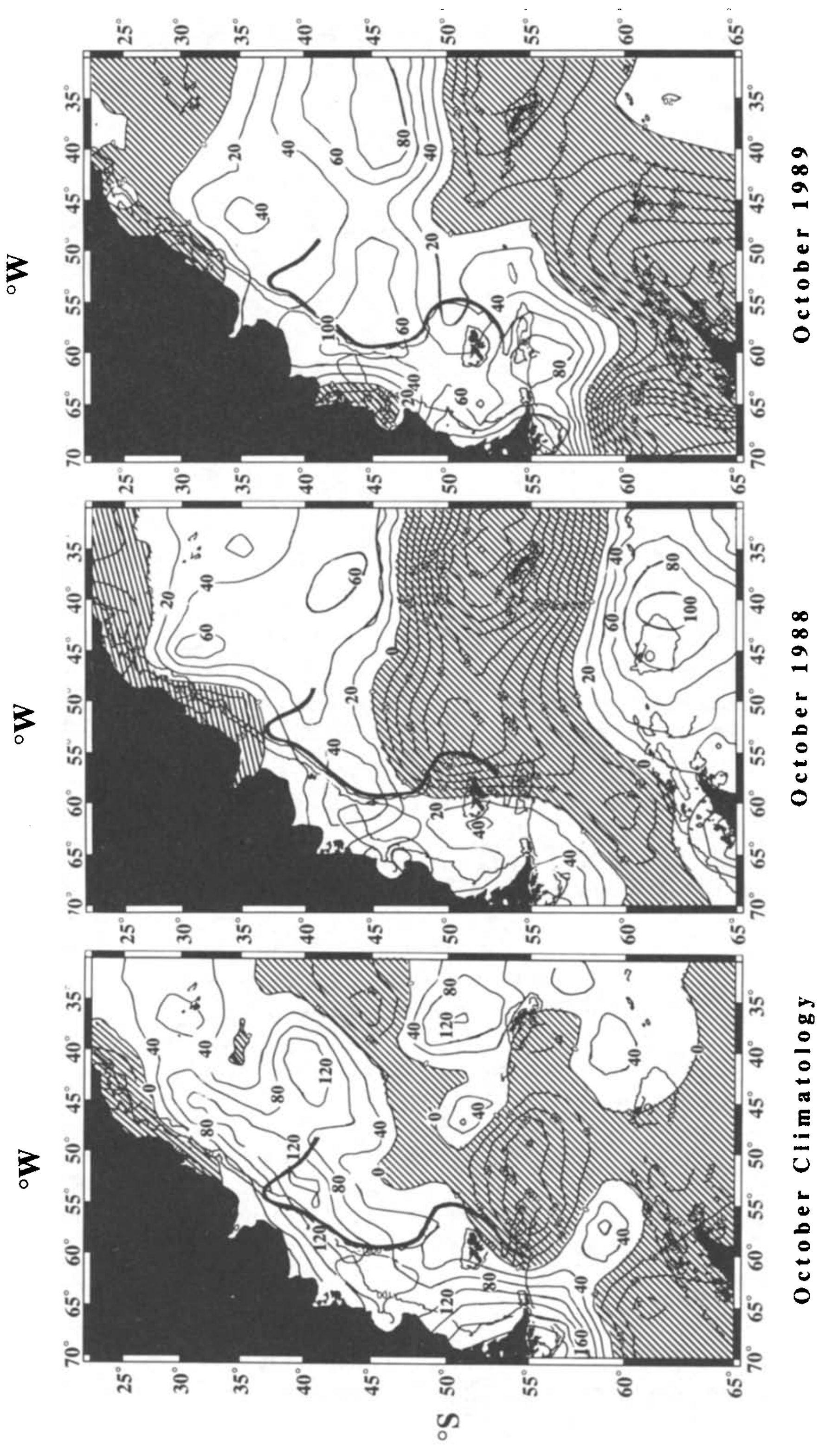

Fig. 10. (a) Climatological map of wind stress curl for the month of October; (b) pseudo curl of the wind stress from the ECW for October 1988 and (c) October 1989. Shaded areas correspond to negative values.

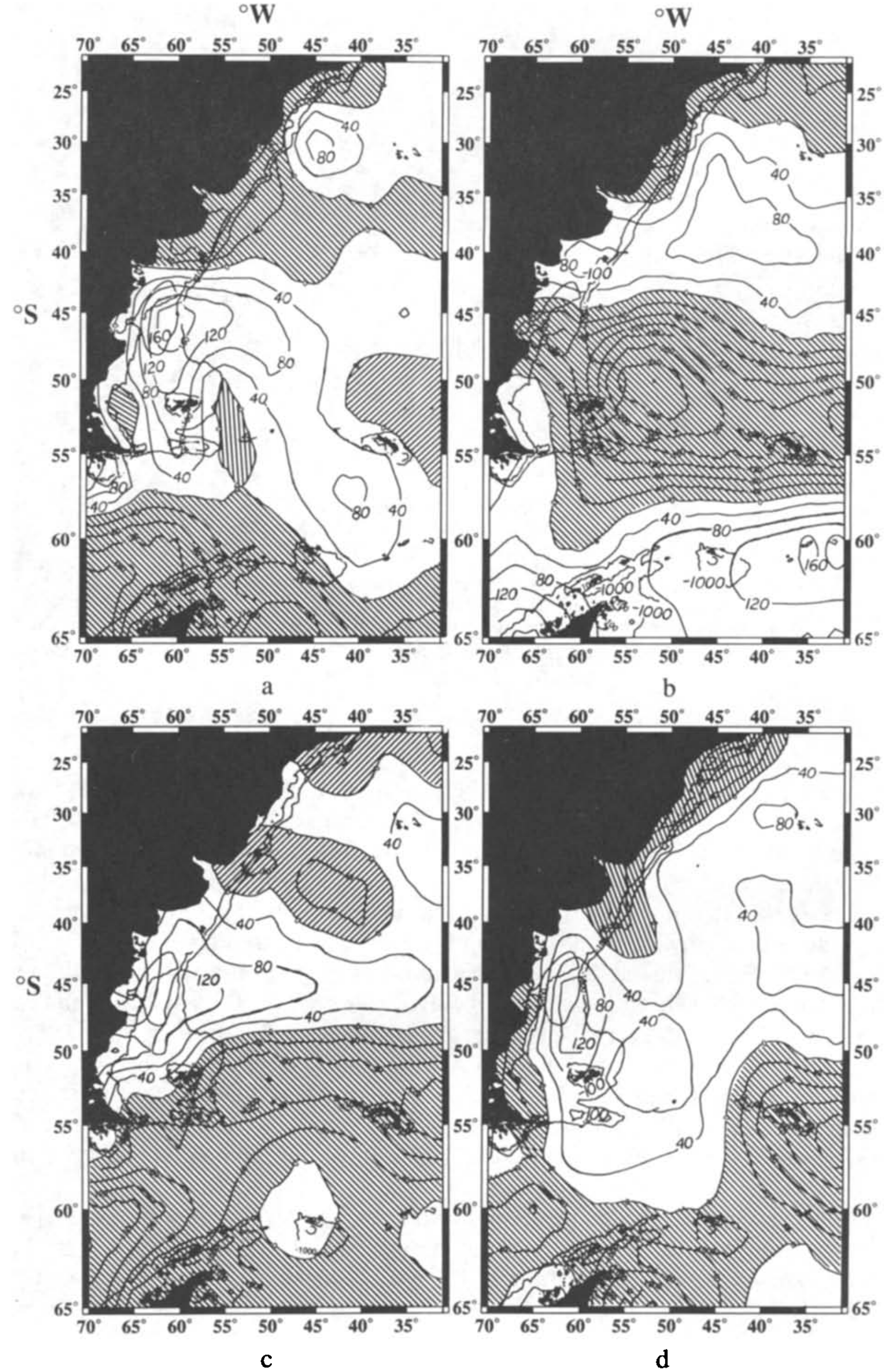

Fig. 11. Pseudo curl of the wind stress from the ECW for: (a) days 1–10 of October 1988; (b) days 21–31 of October, 1988; (c) days 21–31 of November 1988 and (d) days 1–10 of January 1989. Shaded areas correspond to negative values.

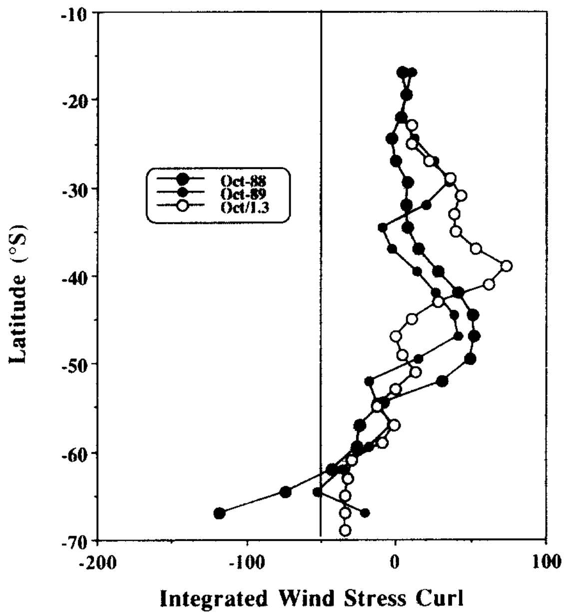

Fig. 12. Curl of the pseudo-wind stress integrated across the South Atlantic basin from the eastern boundary to 70°W for: October 1988 (●), October 1989 (•) and curl of the wind stress from climatology divided by 1.3 (○).

Current reaches its northward location during the SH winter (OLSON *et al.*, 1988; GARZOLI and GARRAFFO, 1989; GARZOLI *et al.*, 1992). Climatological winds indicate that during May, June and July, the positive maximum of the wind stress curl is centered around 30°S (Fig. 5). The zero of the wind stress curl is at its northward location (~45°S). As a consequence, the Brazil Current at the Confluence is weaker. These generate the conditions for the northward penetration of the Malvinas Current.

According to Fig. 2, this description corresponds with the observation for the period May–September 1989 with the exception of July. From 15 to 25 July, at 37.7°S and east of 54°W, the observations indicate the presence of Brazil waters. According to BIANCHI and GARZOLI (1993), this could be due to either an intensification of the Brazil Current or a diminishing of the Malvinas transport, which forces the Malvinas Current to retreat; as satellite images apparently indicate, the Malvinas waters are constrained to a very thin cold tongue west of the deployment lines. In what follows, an explanation will be sought in the wind field.

The differences in the local distribution of wind stress curl from climatology and pseudo wind stress from the ECW wind for the month of July (Fig. 14) are remarkable. Climatology shows negative values for the curl of the wind stress at the Drake Passage and at the base of the Malvinas Current. On the contrary, during July 1989, along the whole extension of the Malvinas Current, as well as in the Drake Passage, the atmospheric motion is dominantly anticyclonic. This will result in an acceleration of the flow counter-clockwise, which will retreat or debilitate the Malvinas Current. To follow further the evolution of this event, the 10-day averages of the pseudo wind stress curl maps are

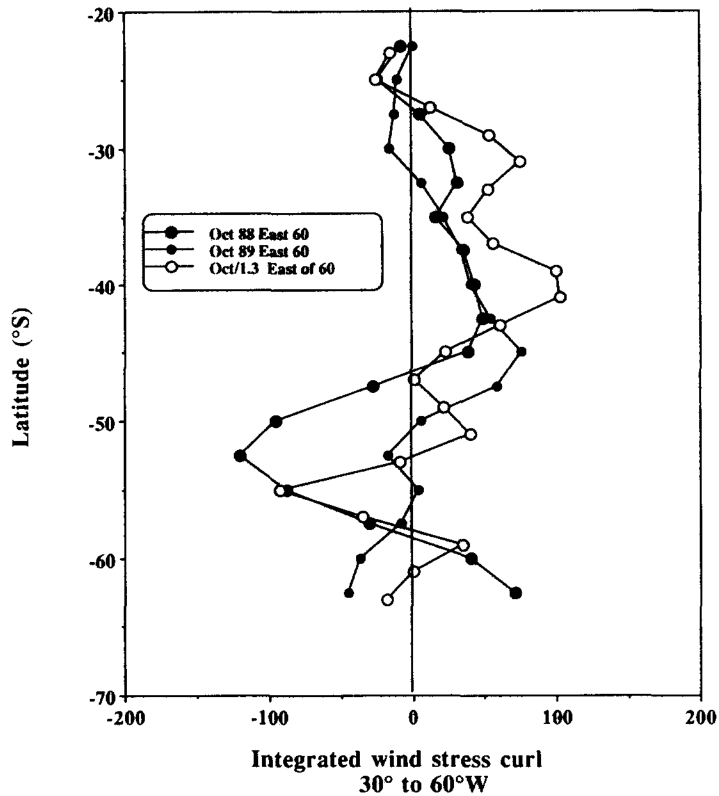

Fig. 13. Curl of the pseudo-wind stress for October 1988 (●), October 1989 (•) and curl of the wind stress divided by 1.3 for climatology (○) integrated from 30°W to 60°W.

analyzed (Fig. 15). At the beginning of June (days 1–10, 1989; Fig. 15a), the wind patterns are both cyclonic and anticyclonic. The cyclonic motion at the Drake Passage and at the base of the Malvinas Current will propitiate the northward flow. By the end of June (days 21–30, 1989; Fig. 15b), an anticyclonic wind curl pattern starts developing in the area of both currents favoring poleward oceanic motion. By mid-July (days 11–21, 1989; Fig. 15c) the anticyclonic pattern dominates the basin from the Drake passage to the coast of Brazil. This will result in a reinforcement of the Brazil Current towards the south and a diminishment of the Malvinas flow. The consequence is the retreat of the Malvinas Current observed in Fig. 2. This result is confirmed by the results from Garzoli (1993) who found that the maximum transport for the Brazil Current, −26.8 Sv, is observed between IES Stas 7 and 8 during the month of July.

The analysis of the zonally (30°–60°W) integrated curl of the wind stress corroborates that the dominant signal south of 42°S was during 1989 out of phase with climatology (Fig. 16). When the same integration is performed for the whole basin (Fig. 17), the curves are in phase with a difference in latitude of the zero crossing attributed to interannual variability of the winds over the whole Atlantic Ocean. Therefore, it can be concluded that

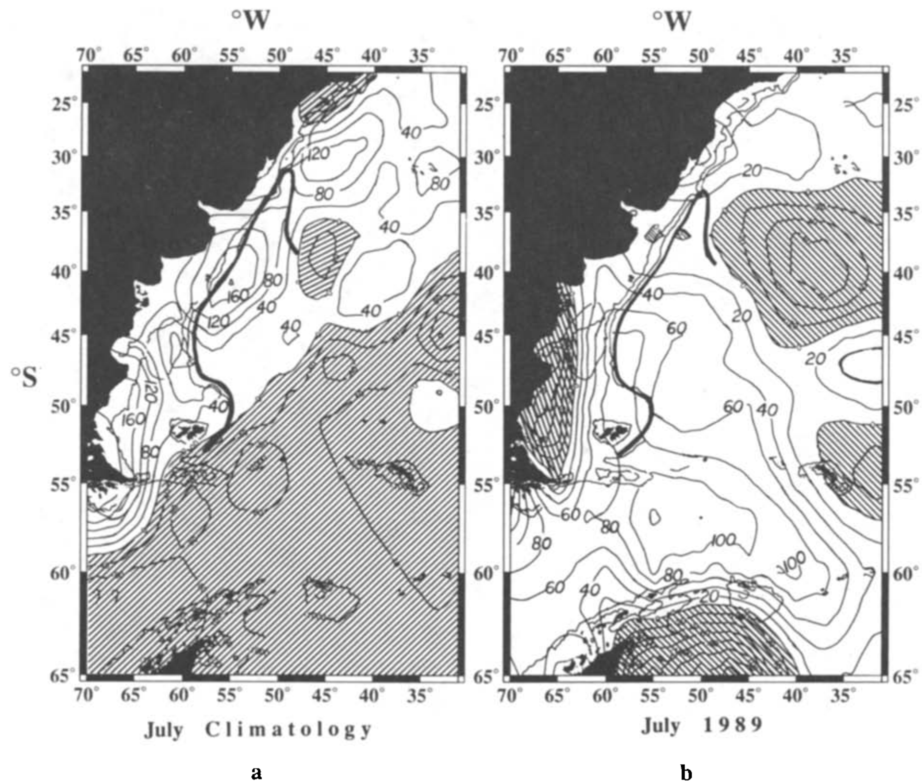

Fig. 14. (a) Climatological map of wind stress curl for the month of July and (b) pseudo curl of the wind stress from the ECW for July 1989. Shaded areas correspond to negative values.

the southward penetration of the Brazil Current during July 1989 is due to an anomalous strong anticyclonic atmospheric motion centered at the location of the Malvinas Current.

5. CONCLUSIONS

The previous discussion leads us to conclude that the main source of variability of the Confluence front is the local wind forcing. There is a variability in the location of the front due to the seasonal cycle of the winds in the South Atlantic. In addition to this seasonal variability, the latitude of separation of the Brazil Current from the coast presents a marked interannual variability that is forced from anomalous wind patterns south of the Confluence. There is no apparent correlation between wind-forced pulses in the Antarctic Circumpolar Current and the observed anomalous northward penetration of the Malvinas Current.

Acknowledgements—Data was collected under NSF grant OCE-87-11529. The present analysis was supported by OCE-91-02541. M. Macció was in charge of the preparation of instruments during deployment and recovery. A. Martino contributed to the computer part of the data reduction and analysis. M. Colwell contributed to the preparation of the final manuscript. L. Ratray prepared the figures for publication. Special thanks to Drs Z. Garraffo for mot helpful discussions during the course of the work and S. Signorini for reviewing the manuscript. This is LDEO contribution number 5193.

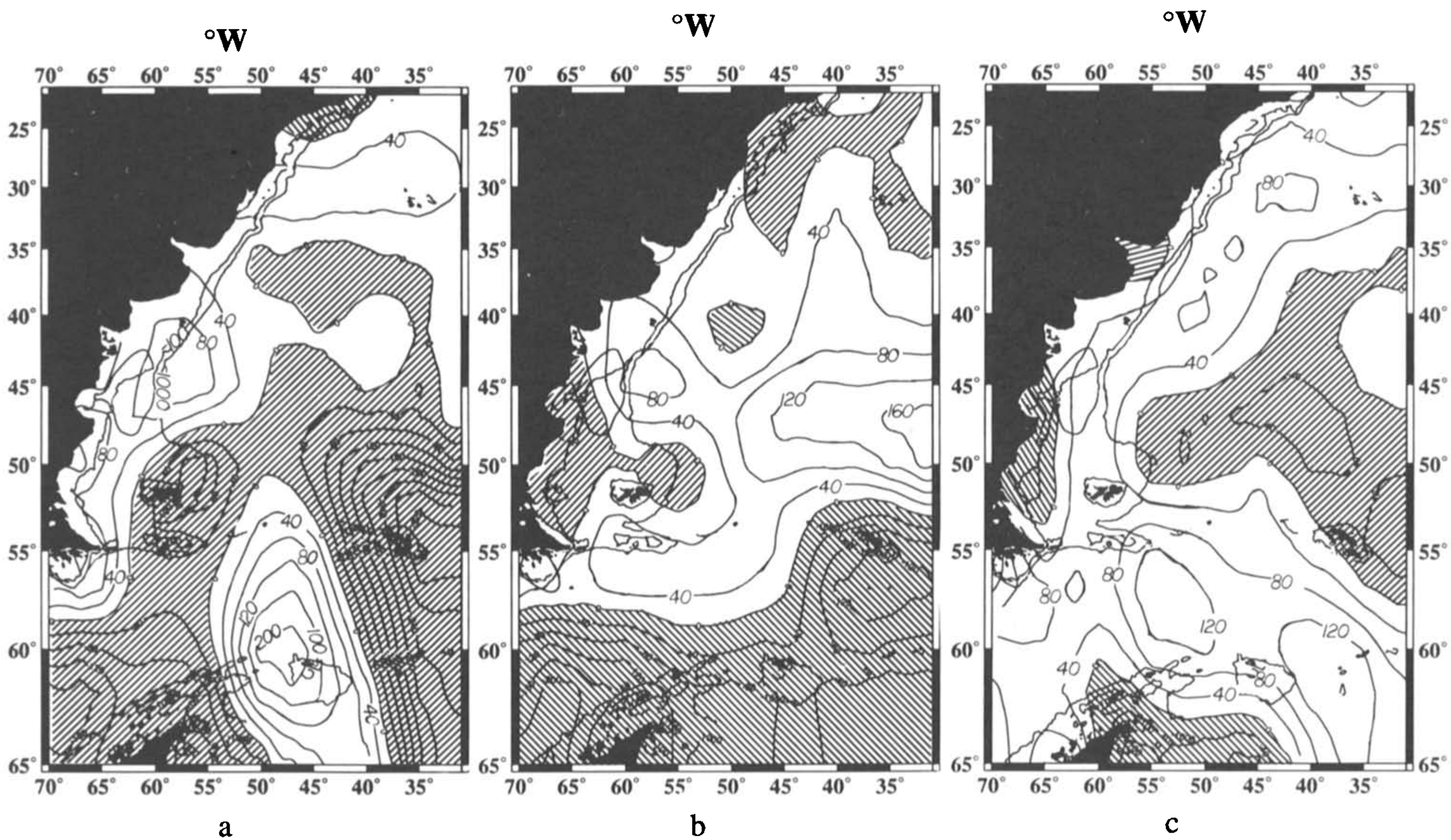

Fig. 15. Pseudo curl of the wind stress from the ECW for: (a) days 1–10 of June 1989; (b) days 21–31 of June 1989; and (c) days 11–20 of July 1989. Shaded areas correspond to negative values.

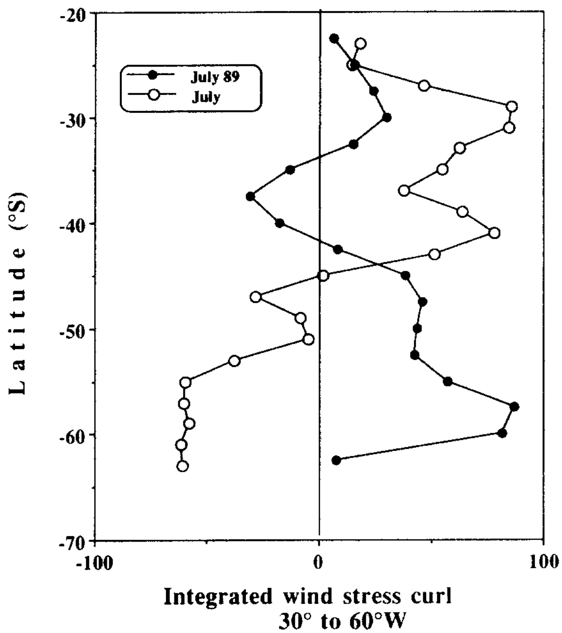

Fig. 16. Curl of the pseudo-wind stress for July 1989 (●) and curl of the wind stress divided by 1.3 for climatology (○) integrated from the eastern boundary to 60°W.

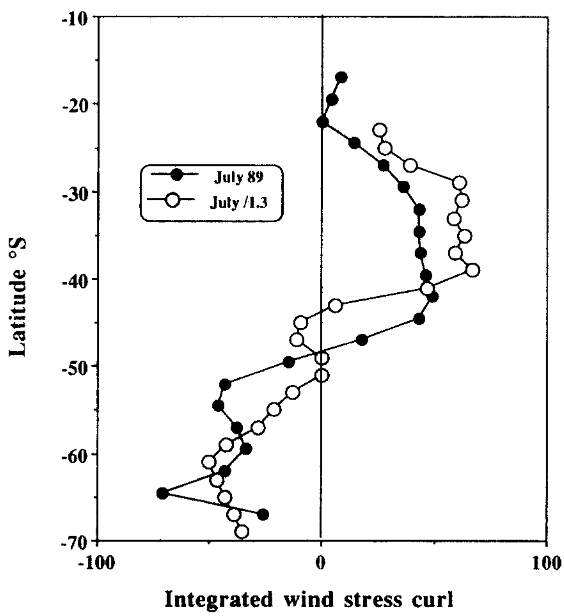

Fig. 17. Curl of the pseudo-wind stress for July 1989 (●) and curl of the wind stress divided by 1.3 for climatology (○) integrated across the South Atlantic basin from 30°E–70°W.

REFERENCES

BIANCHI A. A. and S. L. GARZOLI (submitted) A description of the variability and motion of the Brazil–Malvinas Confluence front. *Deep-Sea Research.*

BIANCHI A. A., C. F. GIULIVI and A. A. PIOLA (1993) Mixing in the Brazil/Malvinas Confluence. *Deep-Sea Research*, **40**, 1345–1358.

CHARO M., A. OSIROFF, A. BIANCHI and A. PIOLA (1991) *Datos Físico-Químicos, CTD y XBT.* Camapañas Oceanográficas, Puerto Deseado 02-88, Confluencia 88 y Confluencia 89, Servicio Hidrografía Naval, Informe Técnico No 59/1991.

CONFLUENCE P.I. (1990) CONFLUENCE 1988–1990: An intensive study of the southwestern Atlantic. *EOS Transactions, American Geophysical Union*, **71**, (41), October.

EVANS D. L., D. R. WATTS, D. HALPERN and S. BOURASSA (1984) Oceanic winds measured from the sea floor. *Journal of Geophysical Research*, **89**(3), 3457–3461.

EVANS D. L. and S. S. SIGNORINI (1985) Vertical structure of the Brazil Current. *Nature*, **315**, 48–50.

GARZOLI S. L., M. MACCIO, A. MARTINO, M. EDWARDS, A. BIANCHI, M. FERRARIO and M. CHARO (1991) *Confluence* 1988–1990 *Data Report.* Lamont-Doherty Geological Observatory Report number LDGO-91-2.

GARZOLI S. L. (1993) Geostrophic velocities and transport variability in the Brazil/Malvinas Confluence. *Deep-Sea Research*, **40**, 1379–1404.

GARZOLI S. L. and M. CLEMENTS (1986) Indirect Wind Observations in the South Western Atlantic. *Journal of Geophysical Research*, **91**(C9), 10,551–10,556.

GARZOLI S. L. and A. BIANCHI (1987) Time–space variability of the local dynamics of the Malvinas/Brazil Confluence as revealed by inverted echo sounders. *Journal of Geophysical Research*, **92**(C2), 1914–1922.

GARZOLI S. L. and Z. GARRAFFO (1989) Transports, frontal motions and eddies at the Brazil/Malvinas Currents Confluence. *Deep-Sea Research*, **36**(5), 681–703.

GARZOLI S. L., Z. Garraffo, G. Podesta and O. BROWN (1992) Analysis of a general circulation model product: Part 1: The geometry of the GCM in the Brazil/Malvinas and Kuroshio/Oyashio systems. *Journal of Geophysical Research*, **97**(C12), 20,117–20,138.

GARZOLI S. L. and C. SIMIONATO (1990) baroclinic instabilities and forced oscillations in the Brazil/Malvinas confluence front. *Deep-Sea Research*, **37**, 1053–1074.

GORDON A. L. and C. GREENGROVE (1986) Geostrophic circulation of the Brazil–Falkland Confluence. *Deep-Sea Research*, **33**(5), 573–585.

HALPERN D., W. KNAUSS, O. BROWN and F. WENTZ (1992) *An atlas of monthly mean distributions of SSMI surface wind speed, ARGOS buoy drift, AVHRR/2 sea surface temperature, and ECMWF surface wind components during* 1989. JPL Publication 92-17, Pasedena, CA.

HELLERMAN S. and M. ROSENSTEIN (1983) Normal monthly wind stress over the world ocean with error estimates. *Journal of Physical Oceanography*, **13**, 1093–1104.

KAZLNAY E., M. KANAMITSU and W. E. BAKER (1990) Global Numerical Weather Prediction at the National Meteorological Center. *Bulletin, American Meteorological Society*, **71**(10), 1410–1428.

LARGE W. G. and S. POND (1981) Open ocean momentum flux measurements in moderate to strong winds. *Journal of Physical Oceanography*, **11**, 324–336.

LARGE W. G. and S. POND (1982) Sensible and latent heat flux measurements over the oceans. *Journal of Physical Oceanography*, **12**, 464–482.

LEMON D. D., D. M. Farmer and D. R. WATTS (1984) Acoustic measurements of wind speed and precipitation over a continental shelf. *Journal of Geophysical Research*, **89**(C3), 3462–3472.

MACCIO M. (1986) *Data compression algorithms using statistical information of the data source. MSEE Project.* School of Engineering. Columbia University.

MATANO R., M. G. SCHLAX and D. B. CHELTON (submitted) Seasonal variability in the southwestern Atlantic. *Journal of Geophysical Research.*

MATANO R. (in press) Seasonal Variability in the Southwestern Atlantic. *Journal of Geophysical Research*,

OLSON D. B., G. P. PODESTA, R. H. EVANS and O. B. BROWN (1988) Temporal variations in the separation of Brazil and Malvinas Currents. *Deep-Sea Research*, **35**(12), 1971–1990.

PETERSON R. G. and L. STRAMMA (1991) Upper-level circulation in the South Atlantic Ocean. *Progress in Oceanography*, **26**, 1–73.

PETERSON R. G. (1988) On the transport of the ACC through the Drake Passage and its relation to wind. *Journal of Geophysical Research*, **93**, 13,993–14,004.

Semtner A. J. and R. M. Chervin (1992) Ocean general circulation from a global eddy-resolving model. *Journal of Geophysical Research*, **97**, 5493–5550.

Shaw P. T., R. Watts and T. Rossby (1978) On the estimation of oceanic wind speed and stress from ambient noise measurements. *Deep-Sea Research*, **25**, 1225–1233.

Stommel H. (1965) *The Gulf Stream*. University of California Press, Berkeley, CA, 248 pp.

Trenberth K. E. and J. G. Olson (1988a) *Evaluation of NMC global analyses* 1979–1987. NCAR Technical Note NCAR/TN-299+STR, 82 pp.

Trenberth K. E. and J. G. Olson (1988b) *ECMWF global analysis* 1979–1986: *Circulation statistics and data evaluation*. NCAR Tech. Note NCAR/TN-300+STR, 94 pp. plus fiche.

Trenberth K. E. and J. G. Olson (1988c) *Intercomparison of NMC and ECMWF global analyses*: 1980–1986. NCAR Tech. Note NCAR/TN-301+STR, 81 pp.

Trenberth K. V., W. G. Large and J. G. Olson (1989) The effective drag coefficient for evaluating wind stress over the oceans. *Journal of Climate*, **2**(12), 1507–1516.

Watts D. R. and H. T. Rossby (1977) Measuring dynamic heights with inverted echo sounders: results from MODE. *Journal of Physical Oceanography*, **7**, 345–358.

Willebrand J. (1978) Temporal and spatial scales of the wind field over the North Pacific and North Atlantic. *Journal of Physical Oceanography*, **8**, 1080–1094.